ELECTROMAGNETIC FIELD PRODUCED BY A SHOCK WAVE PROPAGATING IN A CONDENSED MEDIUM

V. V. Surkov

UDC 534.222.2

Many researchers have observed the development of an electromagnetic field during shock compression of solids [1, 2]. A current pulse in an external circuit [1] and a signal in a receive antenna [2] have been recorded from the moment of shock wave formation until its exit from the specimen. Electromagnetic perturbations of the terrestrial field have also been observed at the epicenter of earthquakes [3]. This phenomenon was studied in [3-6] for the purpose of predicting earthquakes. The signal spectrum is in the low-frequency range (up to several MHz) and the effect is observed in all materials: metals, dielectrics, semiconductors, plastics, sand, etc., although in some materials the effect shows a threshold character. The effect in question has been explained by movement of various types of structural defects (point defects in [1], dislocations and cracks in [5, 6]), and by electrification of rock during its disintegration [7-9].

The present study will use a model of shock polarization of a material in a shock wave analogous to that of [1]. We will treat an almost spherical shock wave and consider the dependence of the degree of polarization on pressure and broadening of the shock front. The development of the electromagnetic field is caused by polarization currents in the wave front. The signal amplitude will be determined on the surface separating two media (near zone). The form of the signal and features of its spectrum will be studied as functions of polarization relaxation time, shock wave characteristic development time and amplitude, and parameters of the medium.

We will consider an almost spherical shock wave propagating in a weakly conductive semispace. We assume that behind the shock wave front the medium is polarized in the radial direction. The polarization of the medium has a weak asymmetry which may be related, for example, to inhomogeneity of the medium, nonuniform development of cracks, slight asymmetry of the shock wave front, the effect of gravity, etc. Without concretizing the mechanism responsible for polarization of the medium, we will describe the latter by an expression of the form

$$P(r, \theta, t) P_0(r) (1 + \beta \cos\theta)\left(1 - e^{-(t-t_0)/\tau}\right) e^{-(t-t_0)/\tau_p} \eta(t - t_0), \quad (1)$$

where β is a small parameter which takes account of asymmetry relative to some direction: $t_0 = (r - a)/v$ is the moment of arrival of the shock wave at a given point r, θ; v = const; a is the radius at which charge is formed in the shock wave: $\eta(t - t_0)$ is a unit function: τ and τ_p are characteristic times for development and relaxation of the polarization pulse. We will neglect motion of the medium behind the shock wave front. The amplitude of the polarization $P_0(r)$ in a plane shock wave is approximately proportional to the pressure D on the front, i.e., $P_0 = AD$ [1], where (for example, for NaCl) $A \sim 3 \cdot 10^{-6}$ C/m^2 GPa.

Considering that the peak pressure in a spherical shock wave varies with distance by a power law, we write

$$P_0(r) = AD_*(a/r)^n. \quad (2)$$

Here D_* is the initial pressure on the shock wave front, the exponent $n \gtrsim 2$ for a plastic wave, and $n \gtrsim 1$ for an elastic wave. The duration of the shock wave front τ is inversely proportional to the amplitude of the pressure [10]; therefore we may assume that $\tau = \tau_f (r/a)^n$. The characteristic time $\tau_p \sim 10^{-3}$-10^{-6} sec is apparently determined to a large degree not by the width of the shock wave front, but by the internal material polarization mechanisms. Thus, for polar dielectrics τ_p is the typical time for thermal reorientation of molecular dipoles, for ionic crystals the relaxation is caused by conductivity $\tau_p \sim \varepsilon\varepsilon_0/\sigma$, where σ is the ionic electrical conductivity and ε is the dielectric permittivity.

Moscow. Translated from Zhurnal Prikladnoi Mekhaniki i Tekhnicheskoi Fiziki, No. 1, pp. 29-36, January-February, 1986. Original article submitted September 24, 1984.

0021-8944/86/2701-0025$12.50

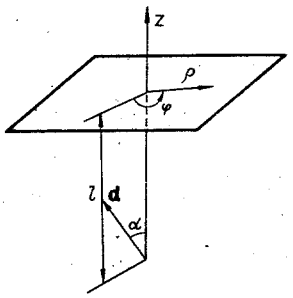

Fig. 1

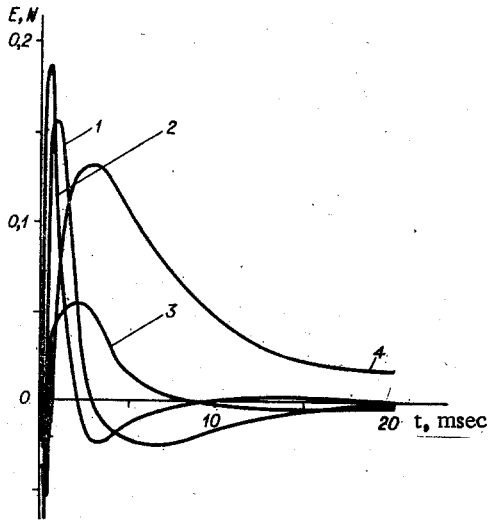

Fig. 2

We will consider the region occupied by the shock wave as an effective radiator. The dipole moment of such a system for $t \geqslant 0$ is directed along some axis of symmetry ($\theta = 0$). The space charge in the source is concentrated mainly near the shock front in a layer of thickness $v(\tau_p + \tau)$, and about a cavity where a compensating charge of opposite sign is found. If the shock wave has yet to reach the surface, then by integrating Eqs. (1), (2) over the volume limited by the radius $r_f = a + vt$ we obtain the dipole moment. Considering that the integral is taken at the length $v(\tau_p + \tau) \ll r_f$, we may assume the functions $r^2P_0(r)$ and $\tau(r)$ within the integral of Eq. (3) to be constant.

As a result,

$$d(t) = \int_V P(r, \theta, t)\cos\theta\, dV = \frac{4\pi\beta AD_* a^n}{3r_f^{n-2}}\left[\tau_p\left(1 - e^{-\frac{t}{\tau_p}}\right) - \tau_*\left(1 - e^{-\frac{t}{\tau_*}}\right)\right],$$
$$\tau_* = \tau_p\tau(rf)/[\tau_p + \tau(rf)]. \tag{3}$$

The symmetric portion of Eq. (1) does not affect dipole moment (3) and produces no contribution to the external field.

We will use the following parameter values: $D_* = 10$ GPa, $a = 10$ m, $\beta = 0.1$, $v = 3\cdot10^3$ m/sec. For these quantities we may assume that the conditions $a/v\tau_p$, $a/v\tau_* \gg 1$ are satisfied. Moreover, at large distances the front becomes sufficiently extended so that the condition $\tau \gg \tau_p$ is satisfied. Considering these facts, we replace Eq. (3) by an approximate expression of the form

$$d(t) = 4\pi B\left[\tau_* e^{-\frac{t}{\tau_*}} - \tau_p e^{-\frac{t}{\tau_p}} + \frac{\tau_p - \tau_*}{(1+t/\tau_m)^m}\right], \quad B = \frac{\beta AD_* a^2 v}{3}, \tag{4}$$

where $\tau_m = a/v$; $m = 2(n-1)$; here and below $\tau_* = \tau_p\tau_f/(\tau_p + \tau_f)$.

Let the distance from the center of the cavity to the surface of the medium be equal to l, while the effective dipole formed by the shock wave forms an angle α with respect to the z axis (Fig. 1). The medium in which the dipole is located is conductive, nonmagnetic ($z < 0$), and is bounded by a vacuum ($z > 0$). We will consider the electromagnetic field at the surface $z = 0$, limiting ourselves to distances ρ (the polar radius) for which the wave numbers $k = \omega/c$ and $\gamma = \sqrt{i\sigma\mu_0\omega}$ satisfy the conditions $k\rho \ll 1$ and $|\gamma|\rho \gg 1$, i.e., we will consider the near zone. These inequalities are valid over the frequency range $(\rho^2\sigma\mu_0)^{-1} \ll \omega \ll c/\rho$. The components of the electromagnetic field were obtained in [11] with consideration of boundary conditions on the surface (polar coordinates):

$$E_к = \frac{\omega d(\omega)e_к}{2\pi\sigma\rho^3} e^{2i\sqrt{i\omega\tau_0}}, \quad H_к = \frac{\omega d(\omega)h_к}{2\pi\gamma\rho^3} e^{2i\sqrt{i\omega\tau_0}},$$
$$e_z = -(\omega\tau_1\cos\alpha + \gamma\rho\sin\alpha\cos\varphi), \quad e_\varphi = -ih_\rho = -2i\sin\alpha\sin\varphi,$$
$$e_\rho = i(\gamma\rho\omega\tau_1\cos\alpha - \sin\alpha\cos\varphi), \quad h_z = 3i\sin\alpha\sin\varphi/\gamma\rho,$$
$$h_\varphi = -(\omega\tau_1\gamma\rho\cos\alpha + \sin\alpha\cos\varphi), \quad \tau_0 = \sigma\mu_0 l^2/4, \quad \tau_1 = \varepsilon_0/\sigma. \tag{5}$$

Here the angle φ is measured from the polar axis on which the dipole moment vector is projected. The dependence of depth l, considered approximately in Eq. (5), transforms to exactness at $\omega\rho \sim c$. The Fourier transform of the dipole moment of Eq. (4) has the form

$$d(\omega) = 4\pi B\left[\frac{\tau_*^2}{1-i\omega\tau_*} - \frac{\tau_p^2}{1-i\omega\tau_p} + (\tau_p - \tau_*)\tau_m \int_1^\infty \frac{e^{i\omega\tau_m(x-1)}}{x^m}\,dx\right]. \tag{6}$$

We will study the features of the frequency spectrum of the signal by substituting Eq. (6) in Eq. (5). The pole terms lead to sharp maxima of $|E_k|$ and $|H_k|$ at $\omega \sim \tau_p^{-1}$ and $\omega \sim \tau_*^{-1}$, and the last term in Eq. (6) gives a marked contribution to the frequency range $\omega \lesssim \tau_m^{-1} \sim 3\cdot 10^2$ sec^{-1}, since in the opposite case there is a rapidly oscillating function within the integral. As $\omega \to 0$ the field vanishes; therefore, in the low-frequency spectral range there may also be a maximum, defined by the characteristic shock wave development time τ_m. If the electrical conductivity of the medium $\sigma = 10^{-2}$–10^{-3} $\Omega^{-1}\text{m}^{-1}$ and $\rho \sim$ 1-10 km, then spectral maxima occur in the frequency interval where Eq. (5) is valid, i.e., in the radio range, as has been confirmed experimentally.

To estimate the signal dependence on time, one can integrate Eqs. (5), (6) over all frequencies, since at low frequencies the fields vanish, and the high-frequency contribution is negligibly small in view of the factor $\exp(2i\sqrt{i\omega\tau_0})$. Thus

$$E_k(\rho, t) = \frac{1}{2\pi}\int_{-\infty}^{\infty} E_k(\rho, \omega)\, e^{-i\omega t}\,d\omega, \tag{7}$$

where E_k and H_k are defined by Eqs. (5), (6). In the region of the maxima the integrand expression $\omega\tau_1 \ll 1$; therefore the field will be produced mainly by the horizontal component of the dipole. The typical integral obtained by substituting the pole terms in Eq. (7) can be written as

$$R_s = \int_{-\infty}^{\infty} \frac{\omega^{s/2}\, e^{(i-1)\sqrt{2\omega\tau_0} - i\omega t}}{1-i\omega\tau_*}\,d\omega,\ s = 0,\ 1,\ 2,\ 3; \tag{8}$$

where the integration contour passes above the branching point $\omega = 0$ and passes through a sheet satisfying the condition of wave attenuation at infinity. We substitute in Eq. (8) the expression

$$\frac{1}{1-i\omega\tau_*} = \int_{-\infty}^{0} e^{y(1-i\omega\tau_*)}\,dy,$$

valid for real ω. Since the integrals are convergent, by changing the order of integration and reducing the frequency range of the inner integrals to the interval 0, $+\infty$, we find

$$\begin{gathered} R_s = \int_{-\infty}^{0} e^{y} Q_s(y, \omega)\,dy, \text{where } Q_0 = 2\int_0^\infty e^{-\sqrt{2\omega\tau_0}}\cos w\,d\omega,\ w = 2\sqrt{\omega\tau_0} - \omega t', \\ Q_1 = (i+1)\int_0^\infty e^{-\sqrt{2\omega\tau_0}}(\sin w + \cos w)\sqrt{\omega}\,d\omega, \\ Q_2 = i\frac{dQ_0}{dt'},\ Q_3 = i\frac{dQ_1}{dt'},\ t' = t + y\tau_*. \end{gathered} \tag{9}$$

With the replacement $z = \sqrt{\omega}$ the integrals Q_0, Q_1 reduce to tabular forms [12]. Then the expressions of Eq. (9) take the form

$$\begin{gathered} R_0 = \frac{2\sqrt{\pi\tau_0}}{\tau_*} e^{-t/\tau_*}\int_0^t e^{t'/\tau_*} L_0(t')\,dt', \\ R_1 = -\frac{(i+1)}{\tau_*}\sqrt{\frac{\pi}{2}}\, e^{-t/\tau_*}\int_0^t e^{t'/\tau_*} L_1(t')\,dt', \\ R_2 = (i/\tau_*)\left[2\sqrt{\pi\tau_0}\,L_0(t) - R_0(t)\right],\ R_3 = (-i/\tau_*)\left[(i+1)\sqrt{\pi/2}L_1(t) + R_1(t)\right], \\ L_0(t) = e^{-\tau_0/t}t^{-3/2},\ L_1(t) = e^{-\tau_0/t}t^{-5/2}(t - 2\tau_0). \end{gathered} \tag{10}$$

The term depending on τ_p is obtained from Eq. (10) by replacing τ_* by τ_p and changing all algebraic signs to their opposites. The integrals of Eq. (10) are more convenient than the original expression (8) and will be used for further analysis.

We will calculate the contribution produced by the last term of Eq. (6). Substituting the latter in Eq. (7) and changing the order of integration (the integrals converge) we obtain

$$T_s^{(m)} = \int_1^\infty \frac{dx}{x^m} \int_{-\infty}^{\infty} \omega^{s/2} e^{(i-1)\sqrt{2\omega\tau_0} - i\omega t''} d\omega, \quad t'' = t - \tau_m(x-1), \quad s = 0, 1, 2, 3. \tag{11}$$

The inner integral in Eq. (11) can be expressed in terms of the functions Q_0, Q_1, Eq. (9).

After similar transformations we have

$$T_0^{(m)} = \frac{2\sqrt{\pi\tau_0}}{\tau_m} \int_0^t \frac{L_0(t')\,dt'}{[1+(t-t')/\tau_m]^m}, \quad T_1^{(m)} = -\frac{(i+1)}{\tau_m}\sqrt{\frac{\pi}{2}} \int_0^t \frac{L_1(t')\,dt'}{[1+(t-t')/\tau_m]^m},$$
$$T_2^{(m)} = \frac{i}{\tau_m}\left[2\sqrt{\pi\tau_0}\,L_0(t) - mT_0^{(m+1)}(t)\right], \quad T_3^{(m)} = -\frac{i}{\tau_m}\left[(i+1)\sqrt{\frac{\pi}{2}}\,L_1(t) + mT_1^{(m+1)}(t)\right]. \tag{12}$$

The components of the electromagnetic field can be expressed in terms of the functions (10), (12):

$$E_z = \frac{(i+1)B}{\pi\rho^2}\sqrt{\frac{\mu_0}{2\sigma}}\sin\alpha\cos\varphi\left[\tau_p^2 R_{3p} - \tau_*^2 R_{3*} - (\tau_p - \tau_*)\tau_m T_3^{(m)}\right],$$
$$E_\rho = \frac{\operatorname{ctg}\varphi}{2}E_\varphi = \frac{iB\sin\alpha\cos\varphi}{\pi\sigma\rho^3}\left[\tau_p^2 R_{2p} - \tau_*^2 R_{2*} - (\tau_p - \tau_*)\tau_m T_2^{(m)}\right],$$
$$H_z = \frac{3B\sin\alpha\sin\varphi}{\pi\sigma\mu_0\rho^4}\left[\tau_*^2 R_{0*} - \tau_p^2 R_{0p} + (\tau_p - \tau_*)\tau_m T_0^{(m)}\right], \tag{13}$$
$$H_\rho = -2\operatorname{tg}\varphi H_\varphi = \frac{(i-1)\sqrt{2}\,B\sin\alpha\sin\varphi}{\pi\rho^3\sqrt{\sigma\mu_0}}\left[\tau_p^2 R_{1p} - \tau_*^2 R_{1*} - (\tau_p - \tau_*)\tau_m T_1^{(m)}\right].$$

At $l = 5\cdot10^2$ m and $\sigma = 10^{-3}\ \Omega^{-1}\text{m}^{-1}$, the parameter $\tau_0 \sim 8\cdot10^{-5}$ sec. In this case the four time parameters defining the features of the signal on the surface lie in the following sequence: $\tau_m \gg \tau_p > \tau_* \gg \tau_0$.

We will study in greater detail the behavior of the component E_ρ, which can be represented as the difference of two terms:

$$E_\rho = E_0\sqrt{\tau_0}\left(N_0 - \frac{m(\tau_p - \tau_*)}{\tau_m}N_{m+1}\right), \quad E_0 = \frac{2B\sin\alpha\cos\varphi}{\sqrt{\pi}\,\sigma\rho^3},$$
$$N_0 = \int_0^t \left(e^{\frac{t'-t}{\tau_p}} - e^{\frac{t'-t}{\tau_*}}\right)L_0(t')\,dt' > 0, \quad N_{m+1} = \int_0^t \frac{L_0(t')\,dt'}{[1+(t-t')/\tau_m]^{m+1}} > 0. \tag{14}$$

In the region $t \ll \tau_*$, expanding the exponentials in the integral N_0 in linear terms, after the change of variables $t' = \tau_0/z^2$ we find

$$N_0 = \frac{1}{\tau_\Phi}\left[\sqrt{\frac{\pi}{\tau_0}}(t + 2\tau_0)\operatorname{erfc}\left(\sqrt{\frac{\tau_0}{t}}\right) - 2\sqrt{t}\,e^{-\tau_0/t}\right]. \tag{15}$$

The term N_{m+1} at $t \ll \tau_m$ leads to the expression

$$N_{m+1} = \sqrt{\frac{\pi}{\tau_0}}\operatorname{erfc}\left(\sqrt{\frac{\tau_0}{t}}\right). \tag{16}$$

Study of Eqs. (15), (16) shows that at $t \ll t_* = \tau_*\tau_p/\tau_m$, $(\tau_p - \tau_*)N_{m+1}/\tau_m \gg N_0$. The signal has an abrupt front with characteristic time τ_0. In the region $t_* \ll t \ll \tau_*$, where $N_0 \gg (\tau_p - \tau_*)N_{m+1}/\tau_m$ a change in sign occurs, and the dependence become linear (Fig. 2, curve 1). The greatest amplitude of the positive phase is reached at $t \sim \tau_*$, τ_p and comprises $E_{max} \sim E_0 \sim \beta AD_* v\alpha^2/\sigma\rho^3$. For the parameter values chosen above we find that $E_{max} \sim 10^9/\rho^3$ μV/m, where ρ is expressed in m.

For $t \gg \tau_p$ in the integral N_0 we perform the replacements $t' = \tau_p z^2$ and $t' = \tau_* z^2$:

$$N_0 = 2\left\{\frac{e^{-t/\tau_p}}{\sqrt{\tau_p}}\int_0^{\sqrt{t/\tau_p}}\frac{e^{z^2-b_p^2/z^2}}{z^2}dz - \frac{e^{-t/\tau_*}}{\sqrt{\tau_*}}\int_0^{\sqrt{t/\tau_*}}\frac{e^{z^2-b_*^2/z^2}}{z^2}dz\right\}, \tag{17}$$

where $b_p^2 = \tau_0/\tau_p$; $b_*^2 = \tau_0/\tau_* \ll 1$. To evaluate the integral, we divide it into two regions. For $z > 1$ only the first term need be retained in the exponent in Eq. (17). For $0 < z < 1$ the integrand has an abrupt maximum at $z \sim b$; therefore, in the given interval the second term of the exponent is significant. Using these approximations and dropping small terms, we obtain

$$N_0 \approx \sqrt{\frac{\pi}{\tau_0}}\left(e^{-t/\tau_p} - e^{-t/\tau_*}\right) + \frac{\tau_p - \tau_*}{t^{3/2}},$$

whence it is evident that in the range $\tau_p \ll t \ll \tau_m$ the signal fails exponentially (with a characteristic time τ_p), and then by a law $t^{-3/2}$, with a change in sign occurring: $(\tau_p - \tau_*) \times N_{m+1}/\tau_m > N_0$. At $t \gtrsim \tau_m$, on the other hand, the value of E_ρ is negative. To estimate the integral N_{m+1} in this region we perform the replacement $t' = \tau_0/z^2$, after which the integral takes on the form

$$N_{m+1} = \frac{2}{\sqrt{\tau_0}\,(1+t/\tau_m)^{m+1}}\int_{\sqrt{\tau_0/t}}^{\infty}\frac{e^{-z^2}z^{2(m+1)}}{[z^2-q^2]^{m+1}}dz, \quad q = \sqrt{\frac{\tau_0}{\tau_m+t}} \ll 1. \tag{18}$$

At $z > 1$ in Eq. (18) we may neglect the parameter q, and in the region $\sqrt{\tau_0}/t < z < 1$ the exponent $\lesssim 1$. We divide the integral of Eq. (18) into two regions with consideration of the simplifications performed above. In this case the answer can be obtained in final form by integration by parts. For integral m, after dropping small terms we have

$$N_{m+1} = \frac{2\left[1 + (\sqrt{\pi}/2)\,\mathrm{erfc}\,(1) + K_{m+1}\right]}{\sqrt{\tau_0}\,(1+t/\tau_m)^{m+1}}, \tag{19}$$

where $K_1 = \frac{1}{2}\sqrt{\frac{\tau_0}{\tau_m+t}}\ln\frac{\sqrt{\tau_m+t}+\sqrt{t}}{\sqrt{\tau_m+t}-\sqrt{t}}$; $K_2 = \frac{\sqrt{\tau_0 t}}{2\tau_m} + \frac{3}{2}K_1$; $K_3 = \frac{\sqrt{\tau_0 t}}{4\tau_m}\left(\frac{9}{2} + \frac{t}{\tau_m}\right) + \frac{15}{8}K_1$.

We note that the expressions obtained are applicable over a wider region: $t \gg \tau_0$, while in the range $\tau_0 \ll t \ll \tau_m$, where the approximation $K_m = m\sqrt{\tau_0 t}/\tau_m\sqrt{2}$ is valid, Eqs. (16), (19) give identical results to the accuracy of a numerical factor ~ 1. Thus, the asymptote of the signal in the region $t \gtrsim \tau_m$ is given by the expression

$$E_\rho = -\frac{2m\,(\tau_p - \tau_*)\,E_0}{\tau_m\,(1+t/\tau_m)^{m+1}}\left[1 + \frac{\sqrt{\pi}}{2}\,\mathrm{erfc}\,(1) + \sqrt{\frac{\tau_0}{2}}\,\tau_m^{-m}\left(\frac{t}{2}\right)^{m-1/2}\right].$$

The maximum modulus of the negative phase is approximately τ_p/τ_m times smaller than the positive and is reached at $t \sim \tau_m$. The characteristic form of the electric E and magnetic H signals is shown in Fig. 2. Calculations were performed for the parameter values given above. Curves 1-4 show the dimensionless functions E_ρ/E_0, $E_z l/E_0\rho$, $3H_\rho l/40H_0\rho$, $H_z/20H_0$, respectively. The region $t < 10^{-3}$ sec, where the functions have peaks or oscillate, must be considered more carefully, since the contribution of high frequencies was considered approximately.

The exit of the shock wave onto the surface, not considered in the present study, leads to appearance of a vertical dipole component. Usually, in this stage the wave transforms to an elastic regime with lower pressures and therefore has no marked effect on the electromagnetic fields.

We will note the role of the scale factor. Thus, if the specimen dimensions are smaller than the relaxation region, the size of which is $\sim v(\tau + \tau_p)$, then the form of the signal presented above changes. The onset of the signal is determined by the time τ_m, and its termination by the relaxation of polarization in the given material or the character of unloading of the specimen surface.

We will consider the component H_z, again dividing the expression into two terms:

$$H_z = \frac{H_0}{\sqrt{\tau_0}}(N_m - S_0), \quad H_0 = \frac{3B\sin\alpha\sin\varphi l^2}{2\sqrt{\pi}\,\rho^4}, \quad S_0 = \int_0^t\left(\tau_p e^{\frac{t'-t}{\tau_p}} - \tau_* e^{\frac{t'-t}{\tau_*}}\right)L_0(t')\,dt', \tag{20}$$

where N_m is defined by an expression analogous to Eq. (14) (for N_{m+1}). For $t \ll \tau_*$ we expand the integrands in Eq. (20) in terms of the parameters $(t - t')/\tau_*$, $(t - t')\tau_p$, $(t - t')/\tau_m$, considering that in the expression for S_0 terms of first order smallness are retained. Integrals of the first nondisappearing terms of the expansion are calculated similarly to Eq. (15). As a result, we have

$$H_z = \frac{H_0}{\sqrt{\tau_0}}\left\{\frac{1}{2\tau_f}\left[\sqrt{\frac{\pi}{\tau_0}}\left(t^2 + 4t\tau_0 + \frac{4}{3}\tau_0^2\right)\operatorname{erfc}\left(\sqrt{\frac{\tau_0}{t}}\right) - \frac{2}{3}\sqrt{t}\,(2\tau_0 + 5t)\,e^{-\tau_0/t}\right] - t_* N_0\right\}, \qquad (21)$$

the expression for N_0 presented in Eq. (15). In the range $\tau_0 \ll t \ll \tau_*$ Eq. (21) takes on the form

$$H_z = \frac{H_0\sqrt{\pi}\,t\,(t - t_*)}{\tau_0\tau_f},$$

whence it is evident that the sign of the function changes.

The maximum value of $|H_z|$ in this region at $t \sim t_*$ is $H_{max} \sim H_0 t_*^2/\tau_0\tau_f \sim \beta A D_* v^3 \tau_*^2 \tau_p^2/\mu_0\sigma\tau_f\rho^4 \sim 10^7/\rho^4$ A/m (ρ expressed in m). At $t > \tau_m$ the falloff of the signal is determined by the asymptote of the expression for N_m. Thus, at $m = 1$ $H_z \sim \ln(t/\tau_m)(1 + t/\tau_m)^{-1}$, while at $m = 2$ $H_z \sim \sqrt{t}/(1 + t/\tau_m)^2$. The maximum value of H_z in the region $t \sim \tau_m$ is approximately τ_m^2/τ_p^2 times larger than H_{max}. The form of the signal is shown by curve 4 of Fig. 2.

Studies revealed that the components E_z and H_ρ behave in a similar manner. Therefore, we will present only asymptotic expressions for $t > \tau_m$. The typical integrals found in the calculations are evaluated like Eqs. (17), (18), by dividing into two intervals. After dropping small values, we obtain

$$E_z = E_0\frac{\rho}{l}\left[\frac{(\tau_p - \tau_*)\sqrt{\tau_0}}{t^{3/2}} + \frac{2m(\tau_p - \tau_*)}{\tau_m(1 + t/\tau_m)^{m+1}}\left\{\frac{\sqrt{\pi}}{2}\operatorname{erfc}(1) - \frac{1}{3} - K_{m+1}\right\}\right],$$

$$H_\rho = H_0\frac{2\rho}{3l}\left[\frac{\tau_p^2 - \tau_*^2}{\sqrt{\tau_0}\,t^{3/2}} + \frac{2(\tau_p - \tau_*)}{\tau_0(1 + t/\tau_m)^m}\left\{\frac{\sqrt{\pi}}{2}\operatorname{erfc}(1) - \frac{1}{3} - K_m\right\}\right].$$

The forward portion of the perturbation for these components may be either monotonic or alternating in sign. This is because the function $L_1(t)$, in contrast to $L_0(t)$, changes sign at $t = 2\tau_0$, and consequently, the contributions to the integral of the regions $t < 2\tau_0$ and $t > 2\tau_0$ can compensate each other. In conclusion, we will present values of amplitudes obtained for $\tau_p - \tau_* = 5\cdot10^{-4}$ sec: $E_z \sim E_0(\tau_p - \tau_*)\rho/l\tau_m \sim 10^6/\rho^2$ μV/m and correspondingly $H_\rho \sim H_0(\tau_p - \tau_*)\rho/l\tau_0 \sim 10^5/\rho^3$ A/m. In contrast to the preceding, the maximum values of these components decrease with the depth of shock wave formation l. Comparison of numerical values shows that at distances $\rho \sim 1$ km all components of the electric vector are of the same order of magnitude, but at large distances E_z decreases more slowly. At $\rho \gtrsim 1$ km the components H_ρ and H_φ are larger than H_z.

The presence in the signal of a short duration peak $\sim\tau_p$, τ_f for all field components is related to the rapid change of the dipole moment in the initial stage of the process. When the size of the relaxation zone becomes small in comparison to the distance traversed by the shock wave the dipole moment changes only because of increase in the volume of the polarized material and decrease in wave amplitude. The decrease in electromagnetic field in this stage is determined by the characteristic mechanical time for shock wave development, i.e., the quantity $\tau_m = a/v$ or r_f/v. Thus, it was established experimentally in [13] that the electromagnetic pulse relaxation time is $\sim W^{1/3}$, where W is the explosion energy. This can be explained by the fact that the quantities a and $r_f \sim W^{1/3}$. The proportionality coefficient coincides with the data of [13], if for r_f we choose the radius of the destruction zone.

The difference in the frequency spectrum is the existence of maxima in the radio range, which agrees with the data of [3-6, 13]. The characteristic length of the electromagnetic wave in this case is much greater than the depth l. This is related to the weak dependence of the peak intensity values on l.

Thus, the effect of mechanical electrification of a condensed medium under the action of a shock wave considered herein permits explanation of experimentally observed principles, in particular, the magnitude and form of the electromagnetic signal on the surface and the frequency spectrum.

In conclusion, the author thanks V. K. Sirotkin and A. S. Chernov for their valuable advice.

LITERATURE CITED

1. V. N. Mineev and A. G. Ivanov, "The emf produced by shock compression of matter," Usp. Fiz. Nauk, 119, No. 1 (1976).
2. Yu. K. Bivin, V. V. Viktorov, et al., "Electromagnetic radiation from dynamic deformation of various materials," Izv. Akad. Nauk SSSR, Mekh. Tverd. Tela, No. 1 (1982).
3. M. B. Gokhberg, V. A. Pilipenko, and O. A. Pokhotelov, "Satellite observations of electromagnetic radiation above the epicentral region of incipient earthquakes," Dokl. Akad. Nauk SSSR, 268, No. 1 (1983).
4. V. M. Demin, G. A. Sobolev, et al., "On the nature of mechanoelectrical radiation of mineral bodies," Dokl. Akad. Nauk SSSR, 260, No. 2 (1981).
5. N. G. Khatiashvili and M. E. Perel'man, "Generation of electromagnetic radiation upon passage of acoustic waves through a cyrstalline dielectric and some mineral ores," Dokl. Akad. Nauk SSSR, 263, No. 4 (1982).
6. M. E. Perel'man and N. G. Khatiashvili, "Generation of electromagnetic radiation by oscillations of twin electric layers and its appearance in earthquakes," Dokl. Akad. Nauk SSSR, 271, No. 1 (1983).
7. V. M. Finkel', Yu. I. Tyalin, et al., "Electrification of alkali halide crystals in the cleaving process," Fiz. Tverd. Tela, 21, No. 7 (1979).
8. M. Ya. Balbachan and E. I. Parkhomenko, "The electret effect in destruction of mineral ores," Izv. Akad. Nauk SSSR, Fiz. Zemli, No. 3 (1983).
9. M. I. Molotskii, "Dislocation mechanism of electrification of ionic crystals during cleavage," Fiz. Tverd. Tela, 18, No. 6 (1976).
10. V. G. Grigor'ev, A. S. Nemirov, and V. K. Sirotkin, "Shock wave structure in elastoplastic relaxing media," Zh. Prikl. Mekh. Tekh. Fiz., No. 1 (1979).
11. J. R. Wait, "The electromagnetic fields of a horizontal dipole in the presence of a conducting half-space," Can. J. Phys., 39, No. 7 (1961).
12. A. P. Prudnikov, Yu. A. Brychkov, and O. I. Marichev, Integrals and Series [in Russian], Nauka, Moscow (1981).
13. C. J. Zablocki, "Electrical transient observed during underground nuclear explosions," J. Geophys. Res., 71, No. 14 (1966).

INDUCTIVE ACCELERATION OF PLANE BODIES

A. M. Abramov, A. A. Blokhintsev,
S. A. Kalikhman, V. I. Kuznetsov,
V. N. Fomakin, and A. A. Tsarev

UDC 538.323:534.2

A promising direction of practical application of the inductive acceleration of plane bodies is the laboratory study of processes occurring in high-velocity collisions. Unlike other methods of studying this process [1], an annular conductor accelerated by electromagnetic forces does not experience the reaction of the accelerating medium and thereby the purity of the experiment is significantly improved.

Processes of high-velocity projection of annular conductors were considered in [2, 3] where the effects of the geometric size of the accelerating system, the resistance, the self-inductance of the energy storage device, and the mass of the accelerated body on the transformation of energy in the accelerator were studied. In [4] analytical expressions and operating curves were obtained, allowing one to choose the optimal regime of acceleration, taking into account the heating of the conductor by the current passing through it. However, because a nonuniform magnetic field acts on the conductor as it speeds up, it is superheated near its inner radius and it deforms and splits. Hence the direct use of a conductor as one of the colliding bodies is limited.

In the present paper we discuss the results of a mathematical model and an experimental study of high-velocity projection of annular conductors when the colliding body is accelerated by another annular conductor. This method can be used to accelerate poorly conducting materials such as steel, titanium, etc., and dielectrics. The experiment was performed for

Cheboksary. Translated from Zhurnal Prikladnoi Mekhaniki i Tekhnicheskoi Fiziki, No. 1, pp. 36-40, January-February, 1986. Original article submitted October 24, 1984.

